DALTON
FULL PAPER

Co-ordination of hydrazine and substituted hydrazines on reaction with $[Rh_2(CO)_4Cl_2]$ and disproportionation of 1,2-$N_2H_2Ph_2$

James V. Barkley, Brian T. Heaton,* Chacko Jacob, Rajeswary Mageswaran and Jeyagowry T. Sampanthar

Department of Chemistry, University of Liverpool, Liverpool, UK L69 3BX

The progressive addition of hydrazine and the following increasingly substituted hydrazines L (N_2H_4 **Ia**, H_2NNHMe **Ib**, H_2NNHPh **Ie**, H_2NNMe_2 **Id**, or MeHNNHMe **Ic**) to $[Rh_2(CO)_4Cl_2]$ resulted in the initial formation of $[\{Rh(CO)_2Cl\}_2(\mu\text{-L})]$ **1** followed by the formation of *cis*-$[Rh(CO)_2L(Cl)]$ **2**; analogous mononuclear complexes were formed directly on addition of the more heavily substituted hydrazines Me_2NNMe_2 **IIf** and H_2NNPh_2 **IIg**, but addition of 1,2-$N_2H_2Ph_2$ **IIIh** to $[Rh_2(CO)_4Cl_2]$ resulted in disproportionation of the hydrazine and formation of *cis*-$[Rh(CO)_2(NH_2Ph)Cl]$ **3** and *cis*-$[Rh(CO)_2(PhN{=}NPh)Cl]$ **4**. The above complexes have been spectroscopically characterised by IR and $^{13}C/^{15}N$ NMR measurements. X-Ray structural analysis on $[\{Rh(CO)_2Cl\}_2(\mu\text{-L})]$ (L = H_2NNHMe or MeHNNHMe) confirmed that L adopts a $\mu\text{-}\eta^1:\eta^1$-mode of bonding with a cisoid arrangement of the $Rh(CO)_2Cl$ groups about the N–N bond.

Hydrazine can co-ordinate to metals as a mono- or bi-dentate ligand or as a bridging ligand.[1] Complexes containing hydrazine are of importance because of their involvement in nitrogen fixation[2] and, more recently, because a mixture of $Rh(NO_3)_3{\cdot}3H_2O$–PPh_3–N_2H_4 in MeOH has been found to be a more efficient hydrogenation catalyst than $[Rh(PPh_3)_3Cl]$.[3,4]

For substituted hydrazines similar modes of co-ordination are found but there are fewer, well characterised examples. Thus, unsymmetrically substituted hydrazines always co-ordinate as a monodentate ligand *via* the least substituted nitrogen[1] and there is only one crystallographically characterised example of a bridging unsymmetrically substituted hydrazine, *viz*. $[\{Ru(cod)Cl\}(\mu\text{-H})(\mu\text{-Cl})(\mu\text{-}\eta^1:\eta^1\text{-}NH_2NMe_2)\text{-}\{Ru(cod)H\}]$;[5] for symmetrically substituted hydrazines there are no crystallographically characterised examples of complexes containing such hydrazines in a bridging mode and only one example of a complex containing such a ligand in a terminal mode, *viz*. *trans*-$[Rh(PPh_3)(MeHNNHMe)Cl_4]^-$.[6]

We now report on the reaction products of $[Rh_2(CO)_4Cl_2]$ with sequential addition of progressively substituted hydrazines (see Scheme 1).

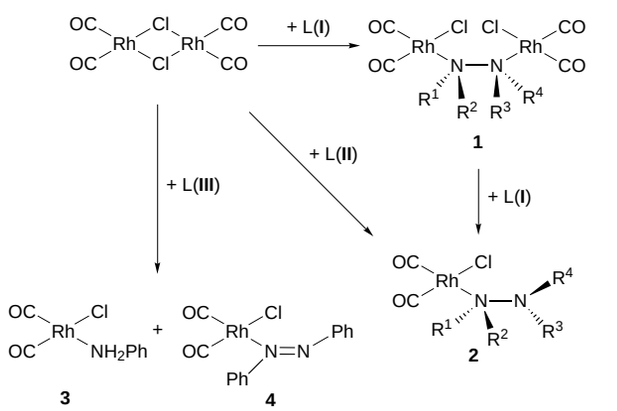

Scheme 1 Reaction products resulting from addition of hydrazine and increasingly substituted hydrazines (L) to $[Rh_2(CO)_4Cl_2]$. Abbreviations used for $R^1R^2NNR^3R^4$: **Ia**, $R^1 = R^2 = R^3 = R^4 = H$; **Ib**, $R^1 = R^2 = R^3 = H$; $R^4 = Me$; **Ic**, $R^1 = R^3 = H$; $R^2 = R^4 = Me$; **Id**, $R^1 = R^2 = H$; $R^3 = R^4 = Me$; **Ie**, $R^1 = R^2 = R^3 = H$; $R^4 = Ph$; **IIf**, $R^1 = R^2 = R^3 = R^4 = Me$; **IIg**, $R^1 = R^2 = H$; $R^3 = R^4 = Ph$; **IIIh**, $R^1 = R^3 = H$; $R^2 = R^4 = Ph$

Results and Discussion

The products resulting from the sequential addition of progressively substituted hydrazines, L, to $[Rh_2(CO)_4Cl_2]$ are shown in Scheme 1. For the less heavily substituted hydrazines (**Ia**–**Ie**) there is excellent low-temperature NMR spectroscopic evidence (^{13}C and ^{15}N, see Tables 1 and 2 respectively) that the first formed product is **1** which is maximised at a ratio of $[Rh_2(CO)_4Cl_2]:\mathbf{I} = 1:1$. Thus, for complexes containing symmetrical hydrazines, (**1a** and **Ic**), there are two carbonyl resonances and, using $^{15}N_2H_4$, only the lower-field resonance [δ(CO) 185.4] shows further coupling; as a result, this resonance must be due to the CO *trans* to the hydrazine [$^1J(^{103}Rh{-}^{13}CO)$ 65.8 and $^2J(^{15}N{-}^{13}CO)$ 12.9 Hz] and the $^{15}N\text{-}\{H\}$ resonance of **1a** and **1c** is a single doublet upfield from that of the free hydrazine with $^1J(^{103}Rh{-}^{15}N)$ 11.8 Hz. For complexes containing unsymmetrically substituted hydrazines, **1b**, **1d** and **1e**, there are four carbonyl resonances and two ^{15}N resonances which are all coupled to rhodium. Representative spectra as exemplified by that of **1b** are shown in Fig. 1.

At room temperature the $^{15}N\text{-}\{^1H\}$ NMR spectra are severely broadened and only one doublet is observed in the ^{13}CO region of the ^{13}C NMR spectrum of complexes **1a**–**1e**. This suggests that the formation of **1** is reversible in solution at room temperature.

It has been possible to obtain X-ray quality crystals of complexes **1b** and **1c** and their structures are shown in Fig. 2. Of interest is the cisoid arrangement of the $Rh(CO)_2Cl$ groups about the N–N bond for both **1b** and **1c** since, although there are no other reported dinuclear structures containing a single bridging substituted hydrazine, all the dinuclear structures containing only a bridging hydrazine are transoid[7–12] and this has been attributed to hydrogen bonding to other ligands on the metal. However, as can be seen in Fig. 2, similar hydrogen bonding interactions can also induce a cisoid arrangement around the N–N bond and all the bond lengths/angles are as expected for a rhodium(I) complex containing a bridging hydrazine with sp^3 N (see Table 3).

Further addition of L (**I**) to complexes **1a**–**1e** produces the monomeric complexes *cis*-$[Rh(CO)_2L(Cl)]$, **2a**–**2e** and spectroscopic measurements show that analogous mononuclear complexes are formed *immediately* on addition of the more sterically demanding ligands, **IIf** and **IIg**. Complex **2f** is the first example containing Me_2NNMe_2 but, in this case, ready

Table 1 Carbon-13 NMR data for $[Rh_2(\mu\text{-}R^1R^2NNR^3R^4)(CO)_4Cl_2]$ complexes

			δ(CO)[a]		^1J(Rh–CO)/Hz	
Compound	*T*/K	Solvent	*a*	*b*	*a*	*b*
1a $[Rh_2(\mu\text{-}NH_2NH_2)(CO)_4Cl_2]$	297	MeOH	183.0 (d)		73.4	
	223		185.4 (d)	180.9 (d)	65.8	74.8
	203		185.6 (d)	181.2 (d)	65.4	74.1
1b $[Rh_2(\mu\text{-}NH_2NHMe)(CO)_4Cl_2]$	297	CH_2Cl_2	180.5 (d)		73.0	
	193		182.5 (d)	178.8 (d)	67.6	75.2
	193	MeOH	185.2 (d)	180.3 (d)	66.9	74.1
1c $[Rh_2(\mu\text{-}MeNHNHMe)(CO)_4Cl_2]$	297	CH_2Cl_2	181.3 (br)			
	193		182.9 (d)	178.8 (d)	68.7	76.3
1d $[Rh_2(\mu\text{-}NH_2NMe_2)(CO)_4Cl_2]$	297	CH_2Cl_2	181.0 (d)		72.5	
	193		181.7 (d)	179.7 (d)	66.6	70.9
1e $[Rh_2(\mu\text{-}NH_2NHPh)(CO)_4Cl_2]$	297	thf	180.9 (br)		*ca.* 72	
	193		184.0 (d)	179.5 (d)	66.9	72.7

d = Doublet, br = broad. [a] CO *trans* to N. [b] CO *cis* to N.

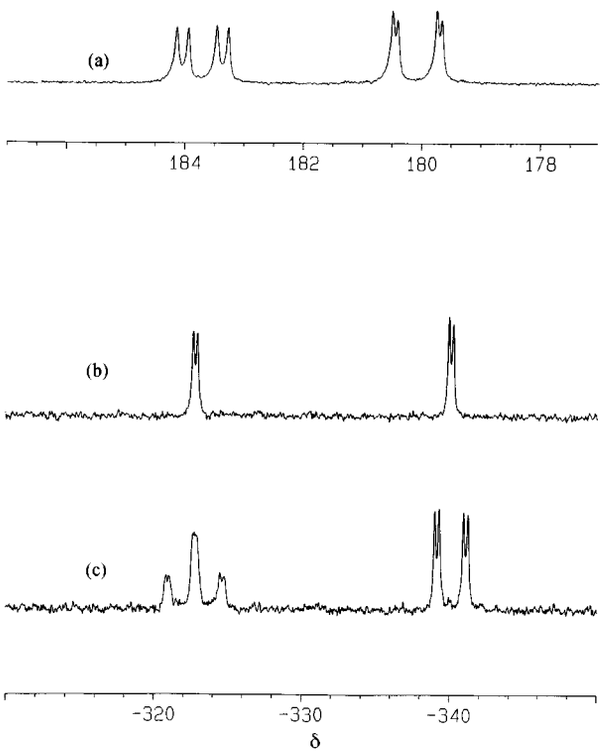

Fig. 1 The NMR spectra of $[\{Rh(CO)_2Cl\}_2(\mu\text{-}\eta^1\text{:}\eta^1\text{-}H_2NNHMe)]$ in CH_2Cl_2 solution at 193 K: (a) $^{13}C\text{-}\{^1H\}$, (b) $^{15}N\text{-}\{^1H\}$ and (c) ^{15}N

decomposition occurs in solution at room temperature presumably because of the proximity of six β-H from the co-ordinated Me_2N groups to the metals.

At room temperature there is only one ^{13}CO NMR resonance for complexes **2a**–**2f** due to the rapid site exchange of L and chloride. However, at low temperature two well resolved carbonyl resonances are observed (Table 4) due to the *cis* configuration and this is consistent with the presence, in all cases, of two equally intense ν(CO) bands in the infrared spectrum. Supporting ^{15}N data for these formulations are reported in Table 2. It should be noted that the ^{13}C NMR spectrum of **2f** at low temperature provides evidence for a major and minor isomer (see Table 4) which, because of steric hinderance, can probably be assigned to the two different rotamers which result from hindered rotation about the N–N bond.

We have previously reported the exclusive rearrangement of 1,2-$N_2H_2Ph_2$ to *o*-semidine (2-$NH_2C_6H_4NHPh$) which becomes catalytic when there are two vacant sites on rhodium.[13] We now find that disproportionation of 1,2-$N_2H_2Ph_2$ **III** occurs on reaction with $[Rh_2(CO)_4Cl_2]$ in CH_2Cl_2 solution to give **3** and **4** in

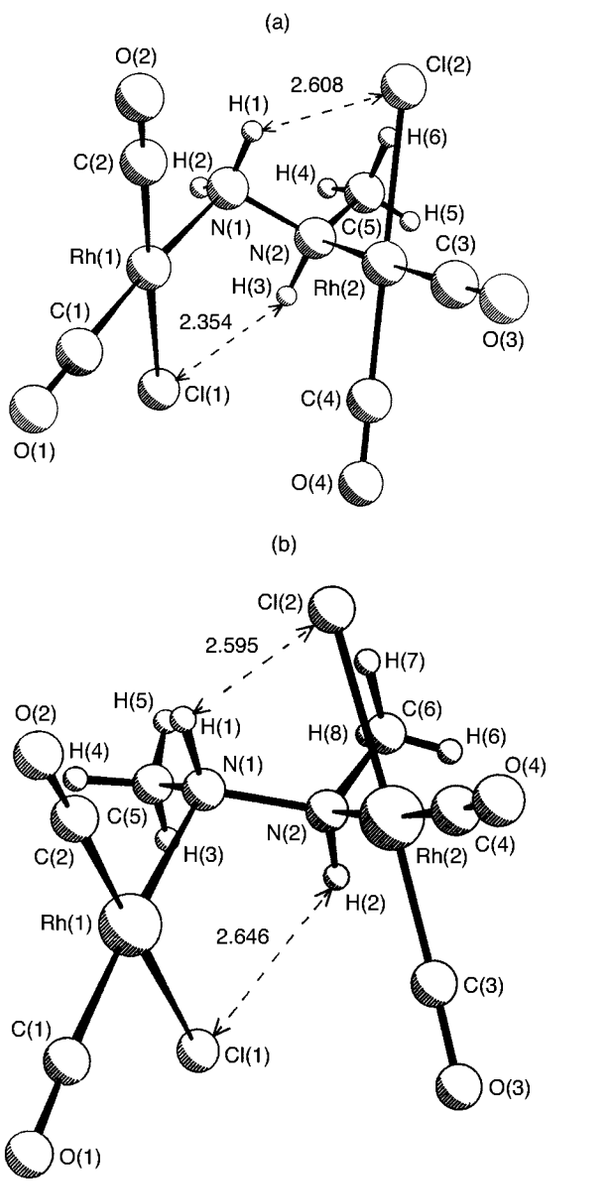

Fig. 2 Schematic representation of the crystal structures (together with the hydrogen-bonding interactions) of: (a) $[\{Rh(CO)_2Cl\}_2(\mu\text{-}\eta^1\text{:}\eta^1\text{-}H_2NNHMe)]$ **1b** and (b) $[\{Rh(CO)_2Cl\}_2(\mu\text{-}\eta^1\text{:}\eta^1\text{-}MeHNNHMe)]$ **1c**

the ratio 2:1 respectively. Both complexes have been prepared independently from the reaction of $[Rh_2(CO)_4Cl_2]$ in CH_2Cl_2 with aniline and azobenzene respectively and, irrespective of

Table 2 ^{15}N INEPT[a] NMR data for rhodium complexes

Compound	*T*/K	Solvent	$\delta(N_\alpha)$[b]	$\delta(N_\beta)$[c]	$^1J(N_\alpha–H)$[b]	$^1J(N_\beta–H)$[c]	$^1J(Rh–N_\alpha)$[b]	$^1J(Rh–N_\beta)$[c]
1a $[Rh_2(\mu\text{-}NH_2NH_2)(CO)_4Cl_2]$	203	MeOH	−350.4 (dt)		73.2		11.8	
1b $[Rh_2(\mu\text{-}NH_2NHMe)(CO)_4Cl_2]$	297	CH_2Cl_2	−321.9 (s)	−340.6 (s)				
	193		−322.9 (dt)	−340.2 (dd)	72.3	75.9	11.0	11.1
1c $[Rh_2(\mu\text{-}MeNHNHMe)(CO)_4Cl_2]$	193	CH_2Cl_2	−326.0 (dd)		79.5		11.8	
1e $[Rh_2(\mu\text{-}NH_2NHPh)(CO)_4Cl_2]$	173	thf	−327.8 (dt)	−321.4 (dd)	74.8	76.9	10.7	11.1
2c $[Rh(CO)_2(MeNHNHMe)Cl]$	193	thf	−326.2 (dd)	−290.3 (d)	79.0	68.0	12.1	
2f $[Rh(CO)_2(Me_2NNMe_2)Cl]$	213	$CDCl_3$	−308.1 (d)	−276.8 (s)			14.9	
2g $[Rh(CO)_2(NH_2NPh_2)Cl]$	213	CH_2Cl_2	−306.3 (dt)	−294.2 (s)	70.7		12.2	
3 $[Rh(CO)_2(NH_2Ph)Cl]$	173	thf	−355.9 (dt)		72.3		10.2	

s = Singlet, dd = doublet of doublets, dt = doublet of triplets; coupling constants in Hz. [a] Insensitive nuclei enhanced by polarisation transfer. [b] N_α = Least substituted N in unsymmetrically substituted hydrazines. [c] N_β = Most substituted N in unsymmetrically substituted hydrazines.

Table 3 Selected bond lengths (Å) and angles (°) for complexes **1b** and **1c**

	1b	**1c**		**1b**	**1c**
Rh(1)–Cl(1)	2.359(1)	2.356(1)	Rh(2)–Cl(2)	2.363(1)	2.346(1)
Rh(1)–N(1)	2.129(4)	2.141(3)	Rh(2)–N(2)	2.147(3)	2.134(3)
Rh(1)–C(1)	1.855(5)	1.837(4)	Rh(2)–C(3)	1.848(5)	1.853(4)
Rh(1)–C(2)	1.854(4)	1.859(4)	Rh(2)–C(4)	1.857(5)	1.862(4)
N(1)–N(2)	1.476(4)	1.474(4)	N(2)–C(5)	1.477(5)	
N(1)–C(5)		1.488(4)	N(2)–C(6)		1.479(4)
Cl(1)–Rh(1)–N(1)	86.1(1)	87.3(1)	Cl(2)–Rh(2)–N(2)	87.7(1)	87.1(1)
Cl(1)–Rh(1)–C(1)	91.5(1)	87.8(1)	Cl(2)–Rh(2)–C(3)	90.7(1)	176.9(1)
Cl(1)–Rh(1)–C(2)	178.1(1)	176.9(1)	Cl(2)–Rh(2)–C(4)	178.2(1)	88.6(1)
N(1)–Rh(1)–C(1)	176.0(2)	175.1(1)	N(2)–Rh(2)–C(3)	178.3(2)	94.6(1)
N(1)–Rh(1)–C(2)	94.4(2)	94.4(1)	N(2)–Rh(2)–C(4)	93.8(2)	175.6(1)
C(1)–Rh(1)–C(2)	87.9(2)	90.4(1)	C(3)–Rh(2)–C(4)	87.9(2)	89.7(2)
Rh(1)–N(1)–N(2)	107.0(2)	105.4(2)	Rh(2)–N(2)–N(1)	106.0(2)	105.6(2)
N(1)–N(2)–C(5)	110.8(3)		Rh(2)–N(2)–C(5)	119.7(3)	
Rh(1)–N(1)–C(5)		114.1(2)	Rh(2)–N(2)–C(6)		115.4(2)
N(2)–N(1)–C(5)		114.4(3)	N(1)–N(2)–C(6)		113.5(3)
Torsion angles					
Rh(1)–N(1)–N(2)–Rh(2)	−50.4(2)	−53.6(1)	O(2)–C(2)–Rh(1)–C(1)	23(5)	30(4)
Rh(1)–N(1)–N(2)–C(5)	178.2(2)		O(3)–C(3)–Rh(2)–N(2)	−73(22)	−152(4)
Rh(1)–N(1)–N(2)–C(6)		179.2(2)	O(3)–C(3)–Rh(2)–C(4)	97(20)	28(4)
Rh(2)–N(2)–N(1)–C(5)		−179.7(2)	O(4)–C(4)–Rh(2)–N(2)	−157(6)	3(10)
Cl(1)–Rh(1)–N(1)–N(2)	−61.1(2)	−63.9(1)	O(4)–C(4)–Rh(2)–C(3)	23(6)	177(9)
Cl(1)–Rh(1)–N(1)–C(5)		62.4(2)	N(1)–N(2)–Rh(2)–C(3)	−77(6)	114.1(2)
Cl(1)–Rh(1)–C(1)–O(1)	46(32)	11(4)	N(1)–N(2)–Rh(2)–C(4)	112.7(3)	−72(2)
Cl(1)–Rh(1)–C(2)–O(2)	−47(8)	−26(6)	N(2)–N(1)–Rh(1)–C(1)	−8(2)	−63(2)
Cl(1)–Rh(2)–N(1)–C(6)		62.8(2)	N(2)–N(1)–Rh(1)–C(2)	117.1(2)	113.5(2)
Cl(2)–Rh(2)–N(2)–N(1)	−66.2(2)	−63.3(2)	C(1)–Rh(1)–N(1)–C(5)		64(2)
Cl(2)–Rh(2)–N(2)–C(5)	60.0(3)		C(2)–Rh(1)–N(1)–C(5)		−120.2(2)
Cl(2)–Rh(2)–C(3)–O(3)	−84(20)	−29(5)	C(3)–Rh(2)–N(2)–C(5)	49(6)	
Cl(2)–Rh(2)–C(4)–O(4)	−16(10)	−6(9)	C(3)–Rh(2)–N(2)–C(6)		−119.7(2)
O(1)–C(1)–Rh(1)–N(1)	−7(34)	9(5)	C(4)–Rh(2)–N(2)–C(5)	−121.1(3)	
O(1)–C(1)–Rh(1)–C(2)	−132(32)	−167(4)	C(4)–Rh(2)–N(2)–C(6)		54(2)
O(2)–C(2)–Rh(1)–N(1)	−154(5)	−149(4)	C(5)–N(1)–N(2)–C(6)		53.0(3)

the method of preparation, there is complete agreement in their spectroscopic properties (see Tables 2 and 5).

Work is continuing to clarify the mechanism of the surprising disproportionation of 1,2-$N_2H_2Ph_2$ and to see how widespread this reaction is.

Experimental

General procedures and materials

The NMR spectra were recorded on either a Bruker WM 200 or AMX 400 spectrometer; ^{13}C, ^{15}N and ^{31}P chemical shifts being referenced to $SiMe_4$, external $MeNO_2$ and to external H_3PO_4 (85% in D_2O) respectively; IR spectra were recorded on a Perkin-Elmer 1720-X Fourier-transform spectrometer in CH_2Cl_2 solution using cells with CaF_2 windows.

Solvents were dried using standard procedures and stored under a nitrogen atmosphere. All manipulations were carried out using Schlenk techniques under a nitrogen atmosphere. Substituted hydrazines were supplied by Aldrich and NH_2NHMe, NH_2NHPh were used as received; MeHNNHMe and NH_2NPh_2 were received as the hydrochloride which were converted into the free hydrazine using the procedure described previously.[14]

Preparation

The dimers $[\{Rh(CO)_2Cl\}_2(\mu\text{-}L)]$ **1a**–**1e** were all prepared by direct stoichiometric addition of L (**Ia**–**Ie**) to a solution of $[Rh_2(CO)_4Cl_2]$ (Rh : L = 2 : 1) under a nitrogen atmosphere. The reaction solvent, recrystallisation solvent together with analytical data, % yield and ν(CO) data of all these products are summarised in Table 6. Further addition of L (**Ia**–**Ie**) to the appropriate dimer (**1a**–**1e**) such that Rh : L = 1 : 1 gave the monomeric complexes *cis*-$[Rh(CO)_2L(Cl)]$ (**2a**–**2e**). Spectroscopic monitoring of the reaction of $[Rh_2(CO)_4Cl_2]$ following the incremental addition of **IIf** or **IIg** produced no evidence for the formation of $[\{Rh(CO)_2Cl\}_2(\mu\text{-}L)]$ but instead showed that *cis*-$[Rh(CO)_2L(Cl)]$ **2f** and **2g** were produced immediately and the yield was maximised at a ratio of Rh : L = 1 : 1. The details are again summarised in Table 6.

Table 4 The ^{13}C NMR data for $[Rh(CO)_2(R^1R^2NNR^3R^4)Cl]$ complexes

			δ(CO)		^1J(Rh–CO)/Hz	
Compound	*T*/K	Solvent	*a*	*b*	*a*	*b*
5a $[Rh(CO)_2(NH_2NH_2)Cl]$	297	MeOH	182.8 (d)		70. 9	
	213		184.6 (d)	181.2 (d)	66. 1	74. 6
5b $[Rh(CO)_2(NH_2NHMe)Cl]$	297	MeOH	181.1 (d)		68.4	
	200		185.0 (br)	180.6 (br)	68.3	72.5
5c $[Rh(CO)_2(MeNHNHMe)Cl]$	297	CH_2Cl_2	182.1 (br)		69.9	
	193		182.9 (d)	179.9 (d)	67.6	75.2
5d $[Rh(CO)_2(NH_2NMe_2)Cl]$	297	CH_2Cl_2	182.1 (br)		*ca.* 61	
	213		182.8 (d)	180.1 (d)	64.3	76.3
5e $[Rh(CO)_2(NH_2NHPh)Cl]$	193	MeOH	184.8 (d)	180.5 (d)	66.4	74.0
	297	thf	184.2 (br)	181.4 (br)	*ca.* 63	*ca.* 71
	173		184.4 (d)	180.8 (d)	66.5	75.2
5f $[Rh(CO)_2(Me_2NNMe_2)Cl]$	300	CH_2Cl_2	180.5 (br)		74.1	
	193		182.6 (d)[c]	179.4 (d)[c]	67.6	78.5
			183.4 (d)[d]	179.8 (d)[d]	67.3	71.9
	300	$CDCl_3$	181.2 (br)			
	213		182.6 (d)[c]	179.9 (d)[c]	67.6	77.4
				180.6 (d)[d]		69.8
5g $[Rh(CO)_2(NH_2NPh_2)Cl]$	300	CH_2Cl_2	181.4 (br)		*ca.* 70	
	213		183.0 (d)	179.3 (d)	67.6	75.2

[a] CO *trans* to N. [b] CO *cis* to N. [c] Major component. [d] Minor component.

Table 5 The ^{13}C NMR data of the products obtained from the reaction of $[Rh_2(CO)_4Cl_2]$ and 1,2-$N_2H_2Ph_2$

			δ(CO)		^1J(Rh–CO)/Hz	
Compound	*T*/K	Solvent	*a*	*b*	*a*	*b*
6 $[Rh(CO)_2(NH_2Ph)Cl]$	297	thf	183.1 (d)		75.3	
	173		185.4 (d)	181.9 (d)	68.3	74.1
	297	MeOH	180.7 (d)		73.0	
7 $[Rh(CO)_2(PhN{=}NPh)Cl]$	297	CH_2Cl_2	178.4 (br)		*ca.* 80.7	
	193		183.2 (d)	178.5 (d)	69.8	73.0

[a] CO *trans* to N. [b] CO *cis* to N.

Table 6 Analytical and infrared, ν(CO), data on rhodium–hydrazine complexes

	Solvent				Analysis[a] (%)			IR	
Complex	Recrystal-lisation	Prepar-ation	Yield (%)	Colour	C	H	N	Solvent	ν(CO)/cm^{-1}
1a $[Rh_2(\mu\text{-}N_2H_4)(CO)_4Cl_2]$	*b*	*b*	61	Light brown	11.5(11.4)	1.1(1.0)	7.0(6.7)	*b*	2089, 2019
1b $[Rh_2(\mu\text{-}NH_2NHMe)(CO)_4Cl_2]$	*c*	*d*	71	Light brown	13.7(13.8)	1.4(1.4)	6.5(6.4)	*c*	2100, 2090, 2029
1c $[Rh_2(\mu\text{-}MeNHNHMe)(CO)_4Cl_2]$	*c*	*d*	72	Light brown	16.1(16.1)	1.8(1.8)	6.3(6.2)	*c*	2099, 2086, 2027
1d $[Rh_2(\mu\text{-}NH_2NMe_2)(CO)_4Cl_2]$	*c*	*d*	64	Dark brown	16.0(16.1)	1.8(1.8)	6.2(6.2)	*c*	2092, 2035
1e $[Rh_2(\mu\text{-}NH_2NHPh)(CO)_4Cl_2]$	*e*	*f*	67	Light brown	24.0(24.2)	1.4(1.6)	5.8(5.6)	*e*	2090, 2019
2a *cis*-$[Rh(CO)_2(N_2H_4)Cl]$	*b*	*b*	88	Brown	10.9(10.6)	2.0(1.8)	12.1(12.4)	*b*	2085, 2017
2b *cis*-$[Rh(CO)_2(NH_2NHMe)Cl]$	*c*	*c*	82	Orange-green	15.0(15.0)	2.6(2.5)	11.6(11.6)	*b*	2084, 2019
2c *cis*-$[Rh(CO)_2(MeNHNHMe)Cl]$	*c*	*d*	72	Light brown	16.1(16.1)	1.8(1.8)	6.3(6.2)	*c*	2099, 2086, 2027
2d *cis*-$[Rh(CO)_2(NH_2NMe_2)Cl]$	*c*	*d*	68	Dark brown	18.8(18.9)	3.1(3.2)	11.3(11.0)	*c*	2089, 2015
2e *cis*-$[Rh(CO)_2(NH_2NHPh)Cl]$	*c*	*c*	72	Red-brown	31.6(31.8)	2.7(2.7)	9.2(9.3)	*b*	2086, 2014
2f *cis*-$[Rh(CO)_2(Me_2NNMe_2)Cl]$	*c*	*d*	63	Dark brown	25.7(25.5)	4.2(4.3)	9.8(9.9)	*c*	2086, 2011
2g *cis*-$[Rh(CO)_2(NH_2NPh_2)Cl]$	*c*	*d*	73	Orange	44.4(44.4)	3.2(3.2)	7.4(7.4)	*b*	2090, 2018

[a] Figures in parentheses are expected results. [b] MeOH. [c] CH_2Cl_2. [d] CH_2Cl_2–light petroleum (b.p. 40–60 °C; 1 : 7). [e] thf. [f] thf–light petroleum (b.p. 40–60 °C; 1 : 7).

Crystallography

Crystal data, data collection and processing details are given in Table 7. All data were recorded on a Rigaku AFC6S diffractometer at −120 °C using graphite-monochromatised Mo-Kα radiation, λ = 0.710 69 Å and 50 KW sealed anode generator, scan width between 1.23 + 0.30 tan θ for **1b** and 1.47 + 0.30 tan θ for **1c**, scan speed 4° min^{-1} for both (two rescans), 2θ = 50°. Three standard reflections were measured every 150 scans; no significant decay was observed. Empirical absorption correction by Ψ scans was applied by the TEXSAN[15] system for **1c** and the maximum and minimum transmission factors are given in Table 7. The unit cells were determined from diffractometer angles for 25 automatically centred reflections with 2θ 39.2–45.5° for **1b** and 48.7–49.8° for **1c**.

Stucture analysis and refinement. Direct methods by full-matrix structure refinement on *F*. All non-hydrogen atoms were treated as anisotropic and hydrogen atoms placed in difference map positions and assigned isotropic thermal parameters 20% greater than the $B_{equivalent}$ value of the atom to which they were bonded. The weighting scheme was based on counting statistics and included a factor ($P = 0.03$) to downweight the intense reflections. Plots of $\Sigma w(|F_o| - |F_c|)^2$ *versus* $|F_o|$, reflection order in data collection, (sin θ)/λ, and various classes of indices

Table 7 Crystal structure analysis, crystal data and experimental details for complexes **1b** and **1c***

	1b	**1c**
Formula	$C_5H_6Cl_2N_2O_4Rh_2$	$C_6H_8Cl_2N_2O_4Rh_2$
M	434.83	448.86
Appearance	Brown, needle	Yellow-orange, prism
a/Å	19.862(3)	22.882(8)
b/Å	11.352(8)	7.725(4)
c/Å	12.400(2)	17.246(6)
β/°	116.57(1)	119.38(2)
U/Å^3	2501(2)	2656(2)
D_c/g cm^{-3}	2.310	2.245
F(000)	1648	1712
μ(Mo-Kα)/cm^{-1}	30.27	28.54
Crystal dimensions/mm	0.200 × 0.200 × 0.300	0.300 × 0.150 × 0.400
Reflections measured	2387	2581
h,k,l Ranges	0–23, 0–13, −13 to 13	0–27, 0–9, −20 to 20
Unique reflections	2316	2511
R_{merg}	0.038	0.025
T_{max}, T_{min}	No absorption correction	1.00, 0.78
Observed reflections [$I > 3.00\sigma(I)$]	1868	2098
Number parameters refined	136	145
R	0.022	0.018
R'	0.028	0.028
Final difference electron-density (maximum, minimum)/e Å^{-3}	0.71, −0.68	0.45, −0.44

* Details in common: monoclinic, space group $C2/c$; $Z = 8$.

showed no unusual trends. The maximum and minimum peaks in the final Fourier-difference map are shown in Table 7. Neutral atom scattering factors were taken from Cromer and Waber.[16] Anomalous dispersion effects were included in F_{calc}.

All calculations were performed using TEXSAN[15] and PLUTO[17] was used for illustrations.

CCDC reference number 186/829.

Acknowledgements

We thank the EPSRC for financial support (to C. J.) and the Royal Society for a Royal Society Third World Fellowship (to R. M.), the Leverhulme Foundation for a Research Fellowship (to B. T. H.) and J. T. S. is grateful for the award of an Overseas Research Scholarship.

References

1 B. T. Heaton, C. Jacob and P. Page, *Coord. Chem. Rev.*, 1996, **154**, 193.
2 M. Hidai and Y. Mizobe, *Chem. Rev.*, 1995, **95**, 1115.
3 W. Heggie, P. R. Page, I. Villax, I. Ghatak and M. B. Hursthouse, Eur. Pat., 0 283 616, 1987.
4 B. T. Heaton, C. Jacob, G. L. Monks, M. B. Hursthouse, I. Ghatak, R. G. Sommerville, W. Heggie, P. R. Page and I. Villax, *J. Chem. Soc.*, *Dalton Trans.*, 1996, 61 and refs. therein.
5 T. V. Ashworth, M. J. Nolte, R. H. Reimann and E. Singleton, *J. Chem. Soc.*, *Dalton Trans.*, 1978, 1043.
6 M. B. Hursthouse, J. Newton, P. R. Page and I. Villax, *Polyhedron*, 1988, **7**, 2087.
7 G. Barrado, D. Miguel, V. Riera and S. Garcia-Granda, *J. Organomet. Chem.*, 1992, **489**, 129.
8 J. A. Broomhead, J. R. Badge, J. H. Enemark, R. D. Feltham, J. I. Gelder and P. L. Johnson, *Adv. Chem. Ser.*, 1977, **162**, 421.
9 P. E. Mosier, C. G. Kim and D. Coucouvanis, *Inorg. Chem.*, 1993, **32**, 2620.
10 D. Sellmann, P. Kreutzer, G. Huttner and A. Frank, *Z. Naturforsch.*, *Teil B*, 1978, **33**, 1341.
11 L.-L. Nguyen, J. Kozelka and C. Bois, *Inorg. Chim. Acta*, 1991, **190**, 217.
12 J. Kozelka, E. Segal and C. Bois, unpublished work quoted in ref. 11.
13 C. J. Davies, B. T. Heaton and C. Jacob, *J. Chem. Soc.*, *Chem. Commun.*, 1995, 1177.
14 C. J. Davies, I. M. Dodd, M. M. Harding, B. T. Heaton, C. Jacob and J. Ratnam, *J. Chem. Soc.*, *Dalton Trans.*, 1994, 787.
15 TEXSAN-TEXRAY, Structure Analysis Package, Molecular Structure Corporation, Houston, TX, 1985.
16 D. T. Cromer and J. T. Waber, *International Tables for X-Ray Crystallography*, Kynoch Press, Birmingham, 1974, vol. 4, Table 2.2A.
17 S. Motherwell and W. Clegg, PLUTO, Program for plotting molecular and crystal structures, University of Cambridge, 1978.

Received 30*th September* 1997; *Paper* 7/07042J